PCCP

Accepted Manuscript

ROYAL SOCIETY OF CHEMISTRY

www.rsc.org/pccp

Which charge definition for describing the crystal polarizing field and the $\chi^{(1)}$ and $\chi^{(2)}$ of organic crystals?†

Tomasz Seidler,*[ab] Benoît Champagne*[a]

Abstract

The impact of atomic charge definition for describing the crystal polarizing electric field has been assessed in view of predicting the linear and nonlinear optical susceptibilities of molecular crystals. In this approach, the chromophores are embedded in the electric field of its own point charges, which are evaluated through a self-consistent procedure including charge scaling to account for the screening of the dielectric. Once the crystal field is determined, dressed molecular polarizabilities and hyperpolarizabilities are calculated and used as input of an electrostatic interaction scheme to evaluate the crystal linear and nonlinear optical responses. It is observed that many charge definitions i) based on partitioning the electron density (QTAIM), ii) obtained by analyzing the quantum-chemical wavefunction (Mulliken, MBS, and NBO), and iii) derived by fitting to the electrostatic potential (MK, CHelpG, and HLYGAt) give very consistent results and are equally valid whereas Hirshfeld partitioning and CM5 charge parametrizations underestimate the refractive indices and second-order nonlinear optical susceptibilities. An alternative approach omitting charge scaling is demonstrated to overestimate the different crystal optical properties. On the other hand, the molecule embedding approach provides results in close agreement with those calculated with a charge field obtained from periodic boundary condition calculations.

keywords: atomic charge definitions, charge embedding approach, self-consistent procedure, linear and second-order nonlinear optical susceptibilities, organic molecular crystals

[a]Laboratoire de Chimie Théorique, University of Namur, rue de Bruxelles, 61, B-5000, Namur, Belgium
[b]Faculty of Chemistry, Jagiellonian University, Romana Ingardena 3, 30-060, Kraków, Poland
Email: tomasz.seidler@unamur.be, benoit.champagne@unamur.be

†Electronic supplementary information (ESI) available: Atomic charges calculated with the B scheme. See DOI: ...

1 Introduction and methodological aspects

There exists a broad list of methods to describe embedding effects in periodic and non-periodic systems. Among these, charge embedding techniques present the advantage of accounting for electrostatic effects at a negligible computational cost. The molecule or region of interest is modeled at a selected quantum mechanical level (QM) and the surrounding is described with the use of classical potential (molecular mechanics - MM) - thus attributing them the QM/MM common name.

These charge embedding schemes have been used in a number of contexts, with the aim of predicting structural, electronic, magnetic, and optical properties. Modeling of the NMR chemical shifts of molecules in single crystals has led to the development of two embedding approaches: the Embedded Ion Method (EIM)[1] and the Surface Charge Representation of the Electrostatic Embedding Potential (SCREEP).[2,3] The EIM method splits the point charge surrounding into three regions: the first comprising $\sim 10^2$ points with charges from *ab initio* calculations, the second spherical around the first ($\sim 10^2$-10^3 *ab initio* charges) and the third with point charges values adjusted in order to reproduce the Ewald potential in the first zone. The SCREEP method mimics the Ewald potential inside the volume surrounding the target molecule with the aid of discretized surface charges. It was shown that by using the NBO charge definition[4] with EIM but the CHelp definition[5] with SCREEP scheme more accurate ^{13}C and ^{15}N NMR chemical shifts are obtained.[6] Weber and auf der Günne[7] presented the Extended EIM (EEIM) scheme where the NBO charge definition is used. At this occasion they reviewed concisely existing approaches for embedding calculations pointing out their limitations. Bjornsson and Bühl devised a computational QM/MM protocol[8] with the aim of improving the X-ray determined geometries of molecular crystals, in view of subsequent simulation of the NMR parameters. The NBO rather than the Merz-Kollman charges fitting the electrostatic potential[9] were recommended whereas severe limitations of the Mulliken charges were shown. The charge embedding technique was also successfully used to model the electron spin resonance parameters (ESR) of oxygen vacancy in semiconducting SnO_2.[10] In that work it was necessary to replace the closest cationic charges by effective core potentials (ECP) in order to prevent charge leakage from cluster to those surrounding charges.

When tackling biological systems, owing to their increased size, QM/MM methods are essential for modeling the interaction energies. It was shown that electrostatically-fitted charges are required to account for polarization effects when describing the interactions between ligands and proteins and therefore for predicting the scoring functions in macromolecular docking.[11] Another QM/MM approach extending the use of point charges for biological applications is the polarizable multipole interaction with supermolecular pairs (PMISP) method.[12] This method decomposes the QM part into smaller subsystems or fragments treating the classical part of the interactions with the use of the polarizable multipole approach. An important issue

when dealing with charged biological systems is the convergence of the atomic charges as a function of the size of QM cluster.[13]

For large molecular systems and crystals, using electrostatic embedding enables to improve the convergence of the many-body expansion of the energy, opening the way to efficient evaluations of their gradient and Hessian.[14] This approach has been employed to predict the relative stability of polymorphs of molecular crystals,[15] one of the most difficult challenges in crystal structures prediction.[16] Charge embedding is also used for modeling solvent effects like in the sequential QM/MM approach that combines Monte Carlo simulations to generate spatial distributions of solute and solvent molecules with *ab initio* calculations of molecular properties.[17,18] For instance, in the same context as this Paper, *i.e.* predicting the nonlinear optical (NLO) properties, this scheme has recently been used to describe the effects of concentration on the first hyperpolarizability of nibrobenzene in benzene[19] and the solvent effects on the first hyperpolarizability of molecular switches.[20] The next step towards improving these QM/MM methods is the use of polarizable embedding. This can be achieved by describing the surrounding at the DFT level of theory while the QM part is treated with correlated wave-function theory (WFT) method, leading to the so-called WFT-in-DFT scheme.[21] This approach has been adopted for calculating the solvatochromic shifts of water in water and uracil in water systems.

In a series of recent papers we have used a charge embedding approach to mimic the inhomogeneous crystal polarizing field for calculating dressed molecular polarizabilities (α) and first hyperpolarizabilities (β).[22–24] Subsequently, these dressed properties were employed within electrostatic interaction schemes to evaluate the macroscopic susceptibilities, $\chi^{(1)}$ and $\chi^{(2)}$. Though this scheme is simplified with respect to *e.g.* EIM, EEIM, or SCREEP and might not be sufficient for predicting NMR parameters, it provides an efficient tool to predict $\chi^{(1)}$ and $\chi^{(2)}$ of organic molecular or ionic crystals. We refer the readers to these papers and references therein for the details on this multiscale procedure. In these studies, the following observations have been made: i) the oscillatory dependence (or slow convergence), as a function of the radius of the sphere containing point charges, of the electric field inside the QM cluster only affects the molecular properties to a small extent and the macroscopic ones even less, ii) imposing the neutrality of the spherical cluster leads to incorrect description of the *in-crystal* polarizing field,[22] and iii) the excess charge shifts the polarizing potential but does not affect the polarizing electric field since the gradient of a constant is zero.[22] So far, in that scheme, only Mulliken charges calculated using periodic boundary conditions (PBC) and the B3LYP exchange-correlation functional were considered. These PBC-derived charges present the advantage of taking into account the *in-crystal* interactions, thus avoiding the use of an iterative approach. Still, in Ref. [22] the impact on $\chi^{(1)}$ and $\chi^{(2)}$ of uniformly scaling the charges by a factor of 0.95 or 1.05 was assessed and found to be small.

In this Paper, to answer the question "Which charge definition is the most suitable for calculating $\chi^{(1)}$ and $\chi^{(2)}$?" several definitions of atomic charges, available in isolated molecule calculations, are employed to describe the crystal polarizing field and the resulting linear and nonlinear optical susceptibilities are compared. The prototypical 2-methyl-4-nitroaniline (MNA) molecular crystal[23] is first chosen for this investigation, which is then extended to two other NLO organic crystals, *m*-nitroaniline (mNA) and *N*-4-nitrophenyl-*L*-prolinol (NPP). Four classes of charges are employed, those resulting from i) partitioning the electron density (Hirshfeld,[25] Bader's quantum theory of atoms in molecules (QTAIM)[26]), from ii) analyzing the quantum-chemical wave-function [Mulliken, minimum basis set Mulliken (MBS),[27] and natural bond orbital (NBO)[4]], from iii) fitting to the electrostatic potential [Merz-Kollman (MK),[9] CHelpG,[5] and Hu-Lu-Yang using standard Gaussian atomic densities (HLYGAt)[28]], and from iv) parametrization to reproduce charge-dependent observable, such as the charge model 5 (CM5), designed to reproduce the dipole moment[29]). The impact of the charge definition is investigated by considering the same levels of approximation as in our previous investigations, *i.e.*, B3LYP/6-311++G(d,p) and MP2/6-311++G(d,p).[22–24] This means that, besides the molecular properties that are calculated at these levels, the charges are also obtained either from B3LYP or MP2 calculations, which leads to four combinations of methods.

Alternatively, within the electrostatic interaction scheme, the dressing effects can be described by a homogeneous dipole field, which takes the form[30]

$$\underline{F}_k = \frac{1}{V\varepsilon_0} \sum_{k'k''} \underline{\underline{D}}_{kk'} \left(\underline{\underline{\alpha}} \left(\omega = 0 \right) \right) \cdot \underline{\underline{L}}_{k'k''} \cdot \underline{\mu}_{k''0} \tag{1}$$

where $\underline{\underline{D}}$ is the local field supertensor [the local field tensor on the k-th (sub)molecule reads $\underline{\underline{d}}_k = \sum_{k'} \underline{\underline{D}}_{kk'}$], $\underline{\underline{L}}$ is the Lorentz dipole-dipole tensor, $\underline{\mu}_{k0}$ is the permanent dipole moment of the k-th (sub)molecule (the molecular dipole moment is equipartitioned over submolecules), and $\underline{\underline{\alpha}}\left(\omega = 0\right)$ the static polarizability supermatrix. An iterative procedure is needed to evaluate the dipole field because the polarizability of the *in-crystal* molecules depend on the dressing field. The derivation of Eq. 1 shows that the self-consistent procedure is done for the (hyper)polarizabilities whereas the dipole moment is fixed to its vacuum value.[31,32] This argument is significant, especially when working with highly polar molecules such as MNA and substantiates the use of a scaling in the self-consistent charge procedure (*vide supra*).

In this Paper, the charged surrounding is a sphere of R=100 $\mathring{A}$ centered on the target molecule. The electric field calculated at the center of nuclear charge as a function of this parameter was shown to be slightly oscillating but not changing much after 60 $\mathring{A}$.[22] The methodology used in this Paper consists of i) calculating - within a given charge definition scheme - the charges of the isolated molecule, of ii) embedding the molecule in a sphere described by these charges, of iii) performing embedded single molecule calculations

to get a new set of charges, and of iv) repeating the calculation of the charges of the target molecule until convergence. Consistently with Eq. 1 a scaling of the charges obtained at the n-th iteration q_i^n is performed based on the atomic charge-derived definition of the dipole moment

$$\underline{\mu}^{q,n} = \sum_i \underline{r}_i q_i^n \tag{2}$$

where the $\underline{r}_i$ are the atomic position vectors. The scaled charges are given by:

$$\tilde{q}_i^n = q_i^n \frac{\left|\underline{\mu}^{q,0}\right|}{\left|\underline{\mu}^{q,n}\right|} \tag{3}$$

The procedure is summarized in a flow chart in Figure 1. The calculations were run to achieve a precision of 10^{-5} e on the atomic charges. In order to show the importance of the charge scaling within the self-consistent charge scheme, an additional set of calculations was conducted omitting the scaling. The two schemes are distinguished by "A", with scaling, and "B", without scaling.

All charge and molecular property calculations were performed with Gaussian09[33] whereas a homemade program was employed to calculate the macroscopic responses.

2 Results and discussion

2.A. Charge distributions and dipole moments of MNA in its crystal field

The MNA structure was taken from neutronographic diffraction data.[34] See Ref. [22] for the representation of the MNA molecule in the abc* axes system. The reference results are considered to be those obtained using Mulliken charges from the PBC-B3LYP/6-31G(d,p) since they were successful for simulating the linear and nonlinear susceptibilities of many different organic crystals.[24] For the A scheme, the calculated atomic charges as obtained with the B3LYP and MP2 methods are gathered in Tables 1 and 2, respectively while in Tables S1 and S2 [ESI†]] for the B scheme. Pearson's correlation coefficients (r) were calculated with respect to the PBC-Mulliken charges. The numbering scheme of Figure 2 was used. The charge-derived (Eq. 2) ($\underline{\mu}^q$) and expectation value dipole moments ($\underline{\mu}$) as well as the angles between these vectors and the *in vacuo* dipole moment ($\underline{\mu}^0$) are provided in Tables 3 and 4 for the B3LYP and MP2 methods, respectively. When using the 6-311++G(d,p) basis set, the single-molecule Mulliken populations are completely different from the reference values (Pearson's r factor is close to 0), and subsequently the angle between $\underline{\mu}^q/\underline{\mu}$ and $\underline{\mu}^0$ is very large. Moreover, the self-consistent procedure diverges if no scaling is applied. This supports severe

limitations of this charge definition with extended basis sets.[35] On the other hand the Mulliken method with a smaller basis set, namely 6-31G(d,p), (referred to further as Mulliken*) provides results very close to those obtained with other methods and its r correlation factor is the largest. The other charge definitions correlate well with the PBC-Mulliken charges, especially MK, MBS, NBO, and HLYGAt. Slightly worse correlations were found for Hirshfeld, CM5, CHelpG, and QTAIM. To address the charge distribution and the associated charge transfer character, since MNA is a push-pull π-conjugated molecule, the atomic charges were summed up into three groups defined as NH_2 (group A), core (group B), and NO_2 (group C). The impact of the charge definition on the group charges is sketched in Figure 3. For all definitions, the core group is the main electron donor to the NO_2 group whereas the charge of the NH_2 moiety is small and either positive or negative, with the exception of QTAIM where it is clearly negative and accepts electrons from the core of the molecule. Several trends are observed, i) the amplitudes of the charges on the B and C moieties are smaller for MK, CHelpG, HLYGAt (which are derived to fit the electrostatic potential), and Hirshfeld but larger for MBS, NBO, and CM5 and even larger for Mulliken* and QTAIM, ii) the self-consistent procedure with charge scaling generally reduces the charge amplitudes on the different molecular moieties whereas the opposite is observed without scaling, iii) to some extent, the differences of charges on the three molecular moieties reflect in the $\underline{\mu}^q$ amplitudes but little in the $\underline{\mu}$ values, which depend less on the charge definition, iv) the B3LYP and MP2 charge distributions on the three moieties are very similar, v) subsequently, the B3LYP and MP2 $\underline{\mu}^q$ amplitudes are much similar, with the exception of the Mulliken* (QTAIM) charge definition where the MP2 values are smaller (larger) than the B3LYP ones, vi) the MP2 and B3LYP expectation value dipole moments are more different than the $\underline{\mu}^q$ values, the MP2 values being the largest, vii) the angle between $\underline{\mu}^q$ or $\underline{\mu}$ and the *in vacuo* dipole moment is very small no matter which charge definition (except Mulliken) and which level of approximation is employed, but viii) the amplitude of the dipole moment increases considerably upon charge embedding. At the MP2 (B3LYP) level of approximation, the increase of the $\underline{\mu}$ amplitude ranges from 23 to 32 % (27 to 38 %) within scheme A whereas it attains 30 to 45 % (43 to 58 %) within scheme B. When compared to $\underline{\mu}$ evaluated with the PBC-Mulliken charge embedding, the other charge definitions lead to smaller dipole moment amplitudes, though the variations remain modest. For instance, at the MP2 level, the reference $\left|\underline{\mu}\right|$ value amounts to 11.39 D, NBO charges underestimate it by 0.2 D, MBS, MK, CHelpG, HLYGAt, and QTAIM by 0.4 D, Mulliken* and CM5 by 0.7 D, and finally Hirshfeld by about 1.0 D. As discussed further, these effects on the amplitudes of the charges and of the dipole moments reflect on the refractive indices and $\chi^{(2)}_{111}$ tensor component of the MNA crystal.

2.B. Refractive indices and second-order NLO susceptibilities of MNA crystal

The n_x refractive index values are presented in Figure 4 while Figure 5 summarizes the results for $-\chi^{(2)}_{111}$ for the different schemes and combinations of methods for evaluating the charges and molecular properties. To analyze the impact of the charge definition, let's consider first the results within scheme A, which deviate negligibly from the 0-th iteration values and then those within scheme B. With the exception of Hirshfeld and CM5 definitions, scheme A values differ very little from the reference results obtained with PBC/B3LYP-Mulliken charges. Still, though remaining small (of the order of 0.01 and 0.02 for QTAIM), these differences are more pronounced when going from the static to the dynamic properties. CM5 and even more Hirshfeld definitions lead to smaller n_x values, by about 0.025 and 0.035, respectively, which is attributed to the corresponding smaller dipole moments. Owing to the absence of scaling and therefore of the larger dipole moments, the scheme B leads to much larger values than those obtained at 0-th iteration whereas the trend when using scheme A is a reduction of n_x with respect to the 0th iteration. Note that combining scheme B with Hirshfeld and CM5 charges leads to good agreement with the reference results, but this should be attributed to error cancellations. Globally, all charge definitions give very similar n_x values, except the Hirshfeld and CM5 schemes.

Similar trends are observed for $\chi^{(2)}_{111}$, though they are usually exalted, which is attributed to the higher order of the response. Thus, scheme A (and also the 0-th iteration method) provides $\chi^{(2)}_{111}$ values very similar to those obtained with the reference charges for all charge definitions, except Hirshfeld and CM5 where the amplitudes are underestimated. Consistently with previous studies,[22,23] the $\chi^{(2)}_{111}$ values are larger when obtained from properties evaluated at the MP2 level than with TDDFT/B3LYP and this difference increases with the photon energy of the incident light.

Though it is not straightforward owing to the many effects that are involved when calculating $\chi^{(1)}$ and $\chi^{(2)}$,[23] a comparison with experiment is helpful. The experimental n_x values amount to 1.953, 2.063, and 2.662 for λ=∞, 1064, and 532 nm, respectively. Figure 4 shows that frequency dispersion is underestimated by the different methods but that charge definition has a negligible impact on this. Indeed, within scheme A, the calculated static values are typically overestimated, the λ=1064 nm values are in good agreement with experiment while at λ=532 nm, the experimental value is underestimated. The impact of this approximate description of frequency dispersion was previously discussed.[23] On the other hand, scheme B leads to larger overestimations of the experimental n_x values, with the exception of λ=532 nm, which is attributed to error cancellations. In the case of $\chi^{(2)}_{111}$, the experimental 300(75) pm/V value[36] is reproduced at most levels of calculation since the experimental standard deviation amounts to 25%. On the other hand, combining scheme B with MP2 molecular properties gives values as large as 650 pm/V, which is well outside the error bars.

2.C. Refractive indices and second-order NLO susceptibilities of other molecular crystals

On the basis of the above results, the linear and nonlinear optical susceptibilities of mNA and NPP were calculated by using two charge definitions, Hirshfeld and CHelpG, which are representative of the behaviors detailed in the previous paragraphs. For both crystals, the neutronographic crystal structures were used (mNA - ref. [37], and NPP - ref. [38]). Like for MNA, the results depend little on the method, B3LYP or MP2, employed for calculating the charges so we selected the later for the discussion. The comparison of the results obtained with different schemes and experiment is provided in Tables 5 and 6, for mNA and NPP, respectively. Note that for mNA, Ref. [39] pointed out limitations of the multiplicative scheme to estimate frequency-dependent (hyper)polarizabilities at the MP2 level, which impedes comparisons of the calculated $\chi^{(2)}_{333}$ quantities with experiment.

The experimental n_x of mNA is well reproduced by all methods, especially when the crystal field is taken into account while the differences between methods to account for the crystal field (including the charge definition) are negligible. On the other hand, n_y is underestimated whereas n_z is overestimated but, globally, the best agreement with experiment is achieved with scheme A. Note that in this case, MP2 gives improved results with respect to B3LYP, where the relative amplitudes of n_y and n_z are inverted.[39] In the case of $\chi^{(2)}_{322}$, the best agreement with experiment is obtained using the PBC-Mulliken charges whereas the differences between schemes A and B are small, in comparison to MNA. Moreover, the differences between the Hirshfeld and CHelpG charge definitions are small and much smaller than in the case of MNA. Still, besides the $\chi^{(2)}_{322}$ = -10.8 pm/V value obtained without accounting for the crystal field, all methods provide results that are consistent with the experimental value and its standard deviation, 23.4 (3.0) pm/V. To some extent, for NPP similar conclusions are drawn, *i.e.* i) neglecting the crystal polarizing field leads to underestimations of the refractive indices (except n_z, which is only weakly impacted by the method of calculation) and $\chi^{(2)}_{112}$, ii) PBC-Mulliken as well as CHelpG (scheme A) charges improve the predictions, iii) CHelpG charges are preferable than Hirshfeld charges, iv) scheme B gives better agreement with experiment than scheme A, especially for $\chi^{(2)}_{112}$ whereas this approach is by construction less rigorous. Again, the standard deviation on $\chi^{(2)}_{112}$ is not negligible and it amounts to 23% of its amplitude (this value was deduced from analogy to $\chi^{(2)}_{112}$ of the similar 2-(*N*-prolinol)-5-nitropyridine (PNP) system, 96(22) pm/V).[39,40]

3 Conclusions

In this paper, several charge definitions to evaluate the *in-crystal* polarizing electric field and thereof the linear and nonlinear optical susceptibilities have been compared by considering the prototypical MNA organic crystal and to a smaller extent mNA and NPP. These include charge definitions i) based on partitioning

the electron density (Hirshfeld, QTAIM), ii) obtained by analyzing the quantum-chemical wavefunction (Mulliken, MBS, and NBO), iii) derived by fitting to the electrostatic potential (MK, CHelpG, and HLYGAt), and iv) defined through parametrizations to reproduce the dipole moment (CM5). The charges of the polarizing field are determined within an iterative procedure where the targeted molecule is embedded in a sphere of point charges. Then, they are used to get the dressed molecular properties and finally the macroscopic optical responses. In the scheme called A, a charge scaling procedure is implemented in order to account for the screening of the charges by the dielectric medium, which corresponds to freezing the static dipole moment to its vacuum value in the dipole field procedure originally proposed by Hurst and Munn.[31] In absence of scaling, the method is referred to as scheme B. The values determined from these self-consistent procedures are compared to those obtained with a charge field obtained from PBC-B3LYP/Mulliken because it has proved to be reliable for a broad set of organic crystals.[24] Results demonstrate i) the better performance of scheme A, as well as of the 0-th iteration scheme, with respect to scheme B, ii) the rather small impact of the choice of charge definition, and iii) still, Hirshfeld and CM5 definitions lead to the largest differences with respect to the other charge definitions, especially in the case of MNA, and to PBC-B3LYP/Mulliken (without emphasizing on the well-known fact that Mulliken charges with too large basis sets also lead to wrong results).

Besides the adequacy of charges derived from PBC calculations, these results demonstrate that i) the crystal polarizing field can also be described by point charges obtained from calculations on the chromophore, embedded in the electric field of its own point charges and that ii) several charge definitions are equally valid to provide reliable linear and nonlinear optical susceptibilities. Note that in the PBC calculations the screening of the charges by the dielectric is implicitly built in the self-consistent procedure providing the wavefunction and band structure whereas in the embedded molecule approach it is built in within a self-consistent procedure including charge scaling. The attractivity of this molecule embedding approach lies in its availability for a broad range of quantum chemistry levels of approximation whereas PBC calculations are available for a more restricted range of methods. Indeed, as illustrated by the applications on MNA, mNA, and NPP through comparisons with experiment, one should keep in mind that such multiscale approach is only reliable provided the molecular properties are evaluated at an adequate level of approximation accounting for electron correlation and frequency dispersion.[23] Note that, like the PBC approach, the charge embedding approach can also account for intermolecular charge transfer effects that occur in crystals containing more than one independent molecule/ion but the situation is more complex than for simple molecular crystals and these issues are beyond the scope of this paper.

ACKNOWLEDGEMENTS

This research was supported in part by PL-Grid Infrastructure as well as by the Belgium government (IUAP N° P7/05, *Functional Supramolecular Systems*). T.S. acknowledges the financial support of IUAP N° P7/05 for his post-doctoral grant. The calculations were performed on the computers of the Consortium des Equipements de Calcul Intensif and mostly those of the Technological Platform of High-Performance Computing, for which we gratefully acknowledge the financial support of the FNRS-FRFC (Conventions No. 2.4.617.07.F and 2.5020.11) and of the University of Namur.

Tab. 1: Atomic charges of the MNA molecule in its crystal environment as obtained within scheme A at the B3LYP/6-311++G(d,p) level of approximation together with Pearson's correlation coefficients (r) with respect to PBC-B3LYP/6-31G(d,p)-Mulliken charges. For a definition of the A-C molecular moieties, see Fig 2.

atom	periodic Mulliken	Mull.* (a)	Mull.* (a) (final)	Mull.	Mull. (final)	MBS	MBS (final)	NBO	NBO (final)	Hirsh.	Hirsh. (final)	CM5	CM5 (final)	MK	MK (final)	CHelpG	CHelpG (final)	HLYGAt	HLYGAt (final)	QTAIM	QTAIM (final)
C1	0.264	0.308	0.235	-1.576	-1.503	0.163	0.131	0.207	0.171	0.067	0.059	0.125	0.104	0.341	0.312	0.418	0.344	0.237	0.251	0.456	0.295
C2	0.096	0.108	0.076	1.786	1.687	-0.024	-0.012	-0.076	-0.044	-0.013	-0.007	-0.023	-0.012	0.204	0.134	0.015	0.006	0.314	0.204	0.010	0.001
C3	-0.143	-0.143	-0.121	-0.189	-0.082	-0.083	-0.065	-0.153	-0.118	-0.034	-0.029	-0.079	-0.062	-0.377	-0.316	-0.199	-0.164	-0.466	-0.384	0.018	0.003
H4	0.127	0.126	0.097	0.216	0.102	0.144	0.106	0.236	0.175	0.054	0.040	0.119	0.088	0.212	0.169	0.158	0.124	0.231	0.185	0.075	0.043
C5	0.209	0.255	0.205	-0.663	-0.122	0.063	0.047	0.032	0.022	0.015	0.010	0.073	0.056	0.100	0.137	0.003	0.026	0.173	0.200	0.277	0.175
C6	-0.106	-0.097	-0.066	0.364	0.073	-0.075	-0.056	-0.157	-0.118	-0.033	-0.027	-0.079	-0.061	-0.274	-0.236	-0.108	-0.099	-0.326	-0.276	0.022	0.020
H7	0.132	0.134	0.094	0.249	0.231	0.151	0.107	0.244	0.176	0.058	0.041	0.121	0.090	0.206	0.162	0.143	0.112	0.219	0.171	0.088	0.039
C8	-0.161	-0.130	-0.123	-0.474	-0.611	-0.139	-0.110	-0.249	-0.196	-0.064	-0.048	-0.111	-0.086	-0.231	-0.198	-0.272	-0.216	-0.197	-0.180	-0.014	-0.013
H9	0.124	0.086	0.101	0.165	0.148	0.104	0.091	0.205	0.168	0.049	0.041	0.107	0.088	0.165	0.138	0.146	0.120	0.169	0.142	0.019	0.053
C10	-0.411	-0.404	-0.321	-0.370	-0.345	-0.267	-0.209	-0.598	-0.462	-0.095	-0.073	-0.238	-0.183	-0.421	-0.291	-0.142	-0.109	-0.500	-0.338	0.021	0.007
H11	0.130	0.130	0.103	0.168	0.124	0.111	0.085	0.222	0.167	0.052	0.041	0.105	0.081	0.145	0.098	0.078	0.053	0.161	0.107	0.022	0.015
H12	0.125	0.125	0.114	0.170	0.104	0.099	0.086	0.208	0.165	0.041	0.038	0.096	0.079	0.128	0.093	0.053	0.047	0.146	0.101	0.004	0.034
H13	0.134	0.116	0.097	0.155	0.192	0.091	0.078	0.205	0.168	0.041	0.035	0.093	0.079	0.100	0.084	0.029	0.035	0.121	0.098	0.002	0.008
N14	-0.646	-0.680	-0.547	-0.274	-0.194	-0.534	-0.406	-0.766	-0.574	-0.163	-0.116	-0.623	-0.470	-0.896	-0.695	-0.890	-0.678	-0.844	-0.667	-1.135	-0.737
H15	0.299	0.275	0.236	0.256	0.183	0.284	0.233	0.389	0.309	0.137	0.116	0.328	0.264	0.401	0.322	0.386	0.309	0.394	0.319	0.392	0.277
H16	0.304	0.276	0.253	0.274	0.234	0.284	0.243	0.396	0.322	0.133	0.117	0.322	0.264	0.403	0.332	0.401	0.329	0.390	0.325	0.397	0.303
N17	0.394	0.359	0.284	-0.206	-0.097	0.362	0.277	0.472	0.364	0.219	0.168	0.051	0.034	0.748	0.530	0.716	0.527	0.720	0.503	0.304	0.191
O18	-0.430	-0.421	-0.358	-0.031	-0.081	-0.368	-0.312	-0.409	-0.345	-0.232	-0.205	-0.195	-0.176	-0.480	-0.388	-0.468	-0.384	-0.473	-0.381	-0.480	-0.359
O19	-0.441	-0.422	-0.359	-0.022	-0.045	-0.366	-0.313	-0.406	-0.351	-0.232	-0.202	-0.194	-0.179	-0.476	-0.388	-0.467	-0.384	-0.467	-0.381	-0.480	-0.354
r coeff.	1.000	0.996	0.998	0.077	0.120	0.981	0.980	0.963	0.968	0.932	0.916	0.907	0.916	0.967	0.970	0.931	0.939	0.958	0.964	0.865	0.878
A	-0.044	-0.129	-0.057	0.257	0.224	0.033	0.070	0.018	0.057	0.107	0.117	0.028	0.058	-0.091	-0.040	-0.102	-0.040	-0.060	-0.023	-0.346	-0.157
B	0.521	0.613	0.490	0.002	-0.002	0.339	0.278	0.325	0.276	0.138	0.122	0.310	0.262	0.299	0.286	0.322	0.281	0.280	0.282	1.003	0.679
C	-0.478	-0.484	-0.433	-0.259	-0.222	-0.372	-0.348	-0.343	-0.332	-0.244	-0.239	-0.337	-0.320	-0.208	-0.246	-0.219	-0.241	-0.219	-0.259	-0.656	-0.521

(a) 6-31G(d,p) basis set

Tab. 2: Atomic charges of the MNA molecule in its crystal environment as obtained within scheme A at the MP2/6-311++G(d,p) level of approximation together with Pearson's correlation coefficients (r) with respect to PBC-B3LYP/6-31G(d,p)-Mulliken charges. For a definition of the A-C molecular moieties, see Fig 2.

atom	periodic Mulliken	Mull.* (a)	Mull.* (a) (final)	Mull.	Mull. (final)	MBS	MBS (final)	NBO	NBO (final)	Hirsh.	Hirsh. (final)	CM5	CM5 (final)	MK	MK (final)	CHelpG	CHelpG (final)	HLYGAt	HLYGAt (final)	QTAIM	QTAIM (final)
C1	0.264	0.354	0.272	-1.718	-1.542	0.231	0.191	0.306	0.261	0.099	0.087	0.157	0.135	0.472	0.430	0.550	0.467	0.365	0.362	0.491	0.365
C2	0.096	-0.055	-0.045	2.084	1.869	-0.055	-0.040	-0.129	-0.092	-0.022	-0.016	-0.032	-0.021	0.122	0.079	-0.077	-0.064	0.233	0.155	0.003	-0.002
C3	-0.143	-0.089	-0.075	-0.206	-0.073	-0.038	-0.031	-0.084	-0.067	-0.010	-0.010	-0.055	-0.046	-0.335	-0.292	-0.154	-0.133	-0.431	-0.366	0.011	0.000
H4	0.127	0.215	0.159	0.272	0.146	0.143	0.108	0.228	0.175	0.058	0.045	0.123	0.095	0.238	0.193	0.183	0.147	0.259	0.211	0.074	0.051
C5	0.209	0.098	0.082	-0.638	-0.195	0.034	0.019	-0.025	-0.031	0.006	0.000	0.064	0.047	0.043	0.085	-0.059	-0.030	0.124	0.154	0.281	0.200
C6	-0.106	-0.079	-0.047	0.278	0.030	-0.027	-0.018	-0.086	-0.063	-0.007	-0.007	-0.053	-0.043	-0.219	-0.199	-0.052	-0.055	-0.275	-0.241	0.014	0.015
H7	0.132	0.222	0.149	0.297	0.256	0.149	0.109	0.236	0.176	0.062	0.046	0.126	0.097	0.229	0.183	0.163	0.131	0.242	0.194	0.087	0.052
C8	-0.161	-0.211	-0.186	-0.519	-0.629	-0.158	-0.132	-0.293	-0.242	-0.074	-0.059	-0.121	-0.098	-0.352	-0.301	-0.386	-0.317	-0.318	-0.283	-0.023	-0.023
H9	0.124	0.158	0.158	0.218	0.194	0.093	0.088	0.197	0.170	0.044	0.039	0.103	0.088	0.197	0.168	0.176	0.148	0.203	0.173	0.031	0.058
C10	-0.411	-0.363	-0.284	-0.453	-0.400	-0.203	-0.165	-0.519	-0.416	-0.081	-0.064	-0.224	-0.178	-0.407	-0.294	-0.101	-0.083	-0.487	-0.345	0.001	-0.004
H11	0.130	0.143	0.110	0.171	0.126	0.090	0.070	0.197	0.153	0.046	0.037	0.099	0.079	0.144	0.100	0.069	0.048	0.159	0.110	0.029	0.019
H12	0.125	0.134	0.119	0.174	0.104	0.078	0.073	0.182	0.152	0.035	0.034	0.089	0.077	0.128	0.097	0.047	0.044	0.146	0.106	0.013	0.033
H13	0.134	0.123	0.105	0.159	0.193	0.069	0.063	0.179	0.153	0.034	0.030	0.086	0.075	0.099	0.085	0.021	0.029	0.120	0.101	0.012	0.014
N14	-0.646	-0.798	-0.629	-0.420	-0.305	-0.589	-0.468	-0.826	-0.654	-0.191	-0.145	-0.650	-0.512	-0.997	-0.808	-0.996	-0.794	-0.943	-0.776	-1.227	-0.920
H15	0.299	0.317	0.264	0.281	0.200	0.285	0.240	0.389	0.320	0.137	0.119	0.328	0.272	0.427	0.353	0.412	0.340	0.419	0.349	0.410	0.320
H16	0.304	0.325	0.289	0.306	0.256	0.288	0.254	0.398	0.336	0.135	0.122	0.324	0.274	0.431	0.366	0.431	0.364	0.417	0.358	0.415	0.343
N17	0.394	0.471	0.368	-0.147	-0.057	0.448	0.358	0.605	0.489	0.284	0.229	0.116	0.091	0.802	0.596	0.780	0.597	0.770	0.566	0.302	0.224
O18	-0.430	-0.483	-0.402	-0.074	-0.102	-0.421	-0.359	-0.479	-0.407	-0.277	-0.245	-0.240	-0.214	-0.513	-0.423	-0.505	-0.420	-0.505	-0.415	-0.463	-0.374
O19	-0.441	-0.483	-0.405	-0.064	-0.070	-0.418	-0.359	-0.475	-0.412	-0.276	-0.242	-0.238	-0.217	-0.508	-0.421	-0.502	-0.419	-0.498	-0.413	-0.463	-0.373
r coeff.	1.000	0.979	0.980	0.133	0.159	0.960	0.959	0.960	0.962	0.904	0.895	0.930	0.935	0.963	0.964	0.902	0.908	0.968	0.969	0.863	0.872
A	-0.044	-0.157	-0.076	0.166	0.150	-0.016	0.026	-0.040	0.003	0.081	0.095	0.002	0.033	-0.139	-0.088	-0.152	-0.090	-0.107	-0.069	-0.401	-0.256
B	0.521	0.653	0.514	0.118	0.078	0.407	0.334	0.389	0.327	0.188	0.163	0.360	0.306	0.359	0.336	0.380	0.332	0.340	0.330	1.025	0.778
C	-0.478	-0.496	-0.438	-0.285	-0.229	-0.391	-0.360	-0.349	-0.330	-0.269	-0.258	-0.362	-0.340	-0.219	-0.247	-0.228	-0.242	-0.233	-0.261	-0.623	-0.522

(a) 6-31G(d,p) basis set

Tab. 3: Charge derived ($\underline{\mu}^q$) and expectation value ($\underline{\mu}$) dipole moments (in Debye), angles (in ^{o}) between these dipole moment vectors and the *in vacuo* dipole moment $\underline{\mu}^0$, and relative increase (in %) of $\left|\underline{\mu}\right|$ with respect to $\left|\underline{\mu}^0\right|$ (last column). All results were obtained at the B3LYP/6-311++G(d,p) level of approximation with either scheme A or B; $\underline{\mu}^0$=[-7.12,2.34,-3.76] D.

charge def.	cycle	μ_x^q	μ_y^q	μ_z^q	$\left\|\underline{\mu}^q\right\|$	$\angle\left(\underline{\mu}^q,\underline{\mu}^0\right)$	μ_x	μ_y	μ_z	$\left\|\underline{\mu}\right\|$	$\angle\left(\underline{\mu},\underline{\mu}^0\right)$	$\frac{\Delta\mu}{\mu^0}$
PBC-Mulliken	-	-8.65	3.12	-4.57	10.27	1.5	-10.01	3.44	-5.29	11.83	0.7	41.1
	0-th	-7.44	2.54	-3.87	8.76	0.7	-9.72	3.42	-5.20	11.54	1.1	37.6
Mulliken* (a)	A	-7.46	2.60	-3.79	8.76	1.4	-9.71	3.30	-5.20	11.50	0.6	37.2
	B	-11.23	3.72	-5.63	13.10	2.3	-11.06	3.69	-5.95	13.09	0.4	56.1
Mulliken	0-th	-7.91	-8.04	-3.49	11.81	59.2	-8.37	0.40	-4.58	9.55	13.8	13.8
	A	-4.89	-10.48	-2.38	11.81	78.8	-7.81	-0.35	-4.27	8.91	18.5	6.3
	0-th	-7.60	2.56	-3.94	8.94	0.6	-9.67	3.26	-5.10	11.40	0.4	36.0
MBS	A	-7.64	2.51	-3.90	8.94	0.8	-9.61	3.20	-5.07	11.33	0.2	35.1
	B	-11.09	3.58	-5.62	12.93	1.0	-10.77	3.59	-5.68	12.69	0.2	51.4
	0-th	-7.93	2.78	-4.27	9.43	1.1	-9.88	3.31	-5.27	11.68	0.3	39.3
NBO	A	-7.98	2.73	-4.22	9.43	0.6	-9.79	3.25	-5.22	11.56	0.3	37.9
	B	-11.71	3.94	-6.13	13.80	0.4	-11.07	3.69	-5.91	13.08	0.3	56.0
	0-th	-6.03	1.92	-3.03	7.02	1.2	-9.04	2.99	-4.76	10.65	0.1	27.0
Hirshfeld	A	-6.06	1.85	-3.01	7.02	1.7	-9.01	2.97	-4.75	10.60	0.1	26.5
	B	-8.43	2.54	-4.17	9.74	1.8	-9.76	3.21	-5.14	11.49	0.1	37.0
	0-th	-6.71	2.13	-3.60	7.90	0.7	-9.29	3.07	-4.97	10.98	0.3	30.9
CM5	A	-6.75	2.10	-3.54	7.90	0.8	-9.25	3.04	-4.93	10.91	0.2	30.2
	B	-9.56	2.94	-4.98	11.17	1.0	-10.16	3.34	-5.43	11.99	0.3	43.0
	0-th	-7.12	2.35	-3.79	8.40	0.1	-9.69	3.21	-5.10	11.41	0.1	36.1
MK	A	-7.13	2.34	-3.77	8.40	0.1	-9.58	3.15	-5.07	11.28	0.1	34.6
	B	-11.64	3.76	-6.14	13.68	0.3	-11.17	3.67	-5.92	13.16	0.1	57.0
	0-th	-7.11	2.37	-3.78	8.39	0.2	-9.71	3.21	-5.09	11.43	0.2	36.3
CHelpG	A	-7.13	2.35	-3.74	8.39	0.1	-9.59	3.15	-5.06	11.29	0.0	34.6
	B	-11.53	3.73	-6.02	13.53	0.3	-11.14	3.66	-5.87	13.11	0.0	56.4
	0-th	-7.09	2.33	-3.77	8.37	0.2	-9.67	3.20	-5.10	11.39	0.1	35.8
HLYGAt	A	-7.09	2.33	-3.78	8.37	0.2	-9.56	3.14	-5.07	11.27	0.1	34.4
	B	-11.60	3.75	-6.17	13.67	0.3	-11.15	3.66	-5.93	13.15	0.2	56.9
	0-th	-8.02	2.63	-4.32	9.48	0.5	-9.80	3.45	-5.13	11.59	1.1	38.2
QTAIM	A	-8.11	2.69	-4.11	9.48	1.0	-9.74	3.34	-5.09	11.49	0.7	37.0
	B	-12.59	4.18	-6.38	14.72	1.0	-11.27	3.92	-5.87	13.30	1.0	58.6

(a) Mulliken charges from B3LYP/6-31G(d,p) calculations

Tab. 4: Charge derived ($\underline{\mu}^q$) and expectation value ($\underline{\mu}$) dipole moments (in Debye), angles (in ^{o}) between these dipole moment vectors and the *in vacuo* dipole moment $\underline{\mu}^0$, and relative increase (in %) of $\left|\underline{\mu}\right|$ with respect to $\left|\underline{\mu}^0\right|$ (last column). All results were obtained at the MP2/6-311++G(d,p) level of approximation with either scheme A or B; $\underline{\mu}^0$=[-7.16,2.37,-3.81] D.

charge def.	cycle	μ_x^q	μ_y^q	μ_z^q	$\left\|\underline{\mu}^q\right\|$	$\angle\left(\underline{\mu}^q,\underline{\mu}^0\right)$	μ_x	μ_y	μ_z	$\left\|\underline{\mu}\right\|$	$\angle\left(\underline{\mu},\underline{\mu}^0\right)$	$\frac{\Delta\mu}{\mu^0}$
PBC-Mulliken	-	-8.65	3.12	-4.57	10.27	1.4	-9.61	3.33	-5.12	11.39	0.7	34.8
	0-th	-7.86	2.76	-4.12	9.29	1.0	-8.98	3.23	-4.91	10.73	1.4	27.0
Mulliken* (a)	A	-7.90	2.74	-4.05	9.29	1.2	-8.96	3.05	-4.90	10.66	0.7	26.1
	B	-11.38	3.87	-5.78	13.34	1.2	-10.24	3.45	-5.62	12.18	0.7	44.1
Mulliken	0-th	-7.23	-9.52	-3.14	12.36	66.8	-7.90	0.11	-4.50	9.09	15.7	7.6
	A	-4.83	-11.13	-2.35	12.36	80.6	-7.61	-0.38	-4.31	8.75	18.9	3.6
	0-th	-7.59	2.59	-3.93	8.93	0.8	-9.34	3.20	-4.94	11.04	0.6	30.7
MBS	A	-7.63	2.55	-3.89	8.93	1.0	-9.30	3.14	-4.93	10.98	0.4	29.9
	B	-10.45	3.45	-5.30	12.22	1.1	-10.11	3.42	-5.35	11.94	0.4	41.3
	0-th	-7.88	2.82	-4.25	9.38	1.2	-9.53	3.23	-5.07	11.27	0.4	33.4
NBO	A	-7.92	2.78	-4.20	9.38	0.9	-9.45	3.18	-5.05	11.17	0.3	32.2
	B	-10.88	3.76	-5.73	12.86	0.8	-10.32	3.48	-5.52	12.21	0.3	44.5
	0-th	-6.15	2.00	-3.09	7.16	1.3	-8.84	2.98	-4.68	10.44	0.3	23.5
Hirshfeld	A	-6.18	1.95	-3.06	7.16	1.6	-8.81	2.95	-4.67	10.40	0.2	23.1
	B	-8.11	2.53	-4.01	9.39	1.8	-9.34	3.13	-4.95	11.02	0.2	30.4
	0-th	-6.82	2.22	-3.66	8.05	0.3	-9.05	3.04	-4.85	10.71	0.3	26.8
CM5	A	-6.85	2.20	-3.60	8.05	0.5	-9.01	3.01	-4.83	10.66	0.2	26.2
	B	-9.15	2.91	-4.78	10.72	0.7	-9.65	3.23	-5.18	11.42	0.3	35.1
	0-th	-7.18	2.39	-3.84	8.48	0.1	-9.38	3.13	-4.96	11.07	0.2	31.0
MK	A	-7.18	2.38	-3.83	8.48	0.1	-9.28	3.08	-4.95	10.96	0.1	29.7
	B	-10.85	3.55	-5.78	12.79	0.2	-10.39	3.44	-5.55	12.27	0.1	45.2
	0-th	-7.16	2.41	-3.83	8.47	0.3	-9.41	3.13	-4.96	11.09	0.2	31.3
CHelpG	A	-7.19	2.39	-3.80	8.47	0.2	-9.31	3.08	-4.94	10.98	0.1	29.9
	B	-10.78	3.53	-5.68	12.68	0.3	-10.39	3.43	-5.52	12.26	0.0	45.1
	0-th	-7.15	2.37	-3.83	8.44	0.2	-9.36	3.12	-4.96	11.04	0.1	30.7
HLYGAt	A	-7.14	2.37	-3.83	8.44	0.2	-9.27	3.07	-4.95	10.94	0.1	29.5
	B	-10.81	3.53	-5.80	12.76	0.3	-10.37	3.43	-5.56	12.26	0.2	45.1
	0-th	-7.31	2.35	-4.02	8.67	0.9	-9.29	3.28	-4.89	11.00	1.1	30.2
QTAIM	A	-7.36	2.48	-3.85	8.67	0.5	-9.23	3.21	-4.87	10.92	0.8	29.3
	B	-11.40	3.79	-5.86	13.37	0.8	-10.39	3.63	-5.47	12.29	1.0	45.4

(a) Mulliken charges from MP2/6-31G(d,p) calculations

Tab. 5: Calculated [MP2/6-311++G(d,p)] versus experimental refractive indices and selected $\chi^{(2)}$ tensor components (in pm/V) for mNA at λ=1064 nm, as determined with different polarizing fields.

method		n_x	n_y	n_z	$\chi^{(2)}_{322}$	$\chi^{(2)}_{333}$
exp		1.690	1.729	1.639	23.4(3.0)	24.6(3.0)
no field		1.681	1.686	1.630	-10.8	-3.2
PBC-Mulliken		1.693	1.701	1.680	-24.6	-10.8
Hirshfeld	0-th	1.688	1.696	1.659	-18.8	-8.7
	A	1.688	1.695	1.658	-18.8	-9.1
	B	1.690	1.698	1.666	-21.4	-10.9
CHelpG	0-th	1.686	1.700	1.667	-19.7	-7.8
	A	1.686	1.699	1.667	-20.2	-8.6
	B	1.689	1.703	1.683	-25.0	-11.5

Tab. 6: Calculated [MP2/6-311++G(d,p)] versus experimental refractive indices and $\chi^{(2)}_{112}$ tensor component (in pm/V) for NPP at λ=1064 nm, as determined with different polarizing fields.

method		n_x	n_y	n_z	$\chi^{(2)}_{112}$
exp		1.931	1.775	1.452	169(39)
no field		1.839	1.717	1.479	55.3
PBC-Mulliken		1.909	1.740	1.475	107.1
Hirshfeld	0-th	1.886	1.732	1.477	87.0
	A	1.886	1.732	1.477	87.1
	B	1.905	1.739	1.476	101.6
CHelpG	0-th	1.904	1.741	1.481	100.9
	A	1.905	1.740	1.479	101.9
	B	1.945	1.754	1.480	136.2

5 Figures

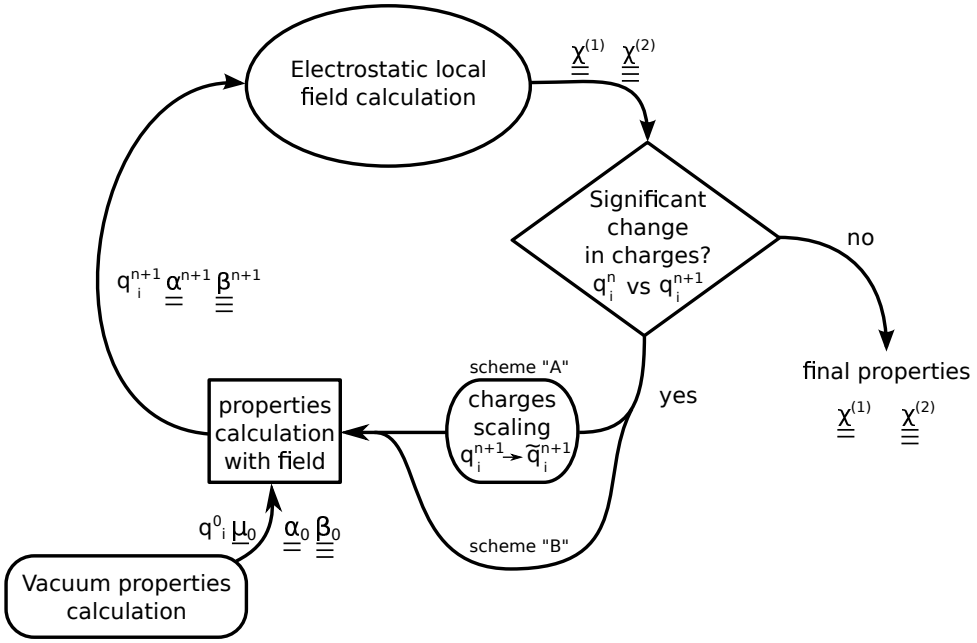

Fig. 1: Flow chart of the charge field self-consistent procedure.

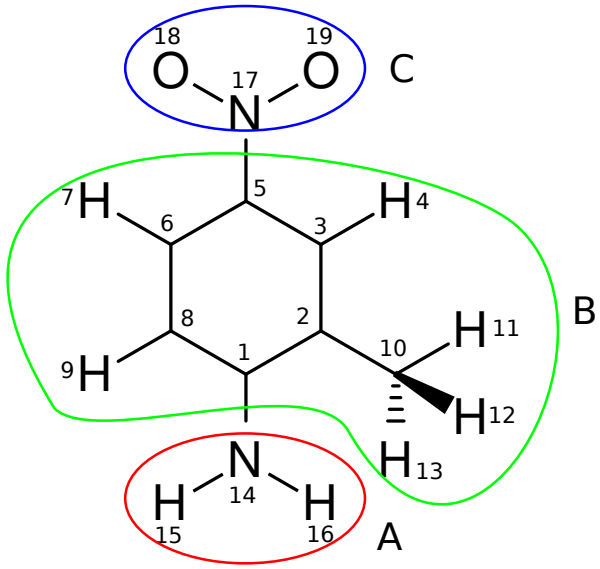

Fig. 2: Numbering scheme used for MNA molecule and its 3 moieties.

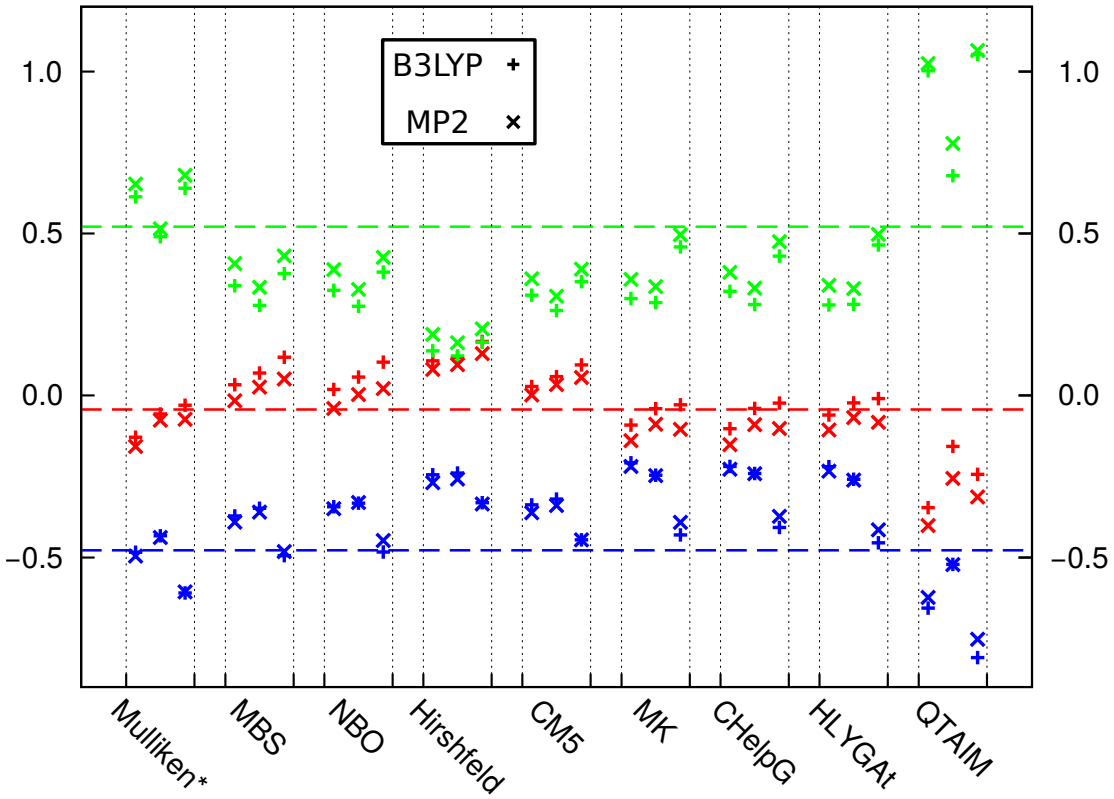

Fig. 3: Charges of moieties A (NH_2 group, red), B (core, green), and C (NO_2, blue) as a function of the charge definition evaluated at the B3LYP and MP2 levels of approximation. For each definition, the 0-th cycle, scheme A, and scheme B values are represented in a sequence from left to right; horizontal dashed lines represent the values obtained with the PBC-Mulliken approach.

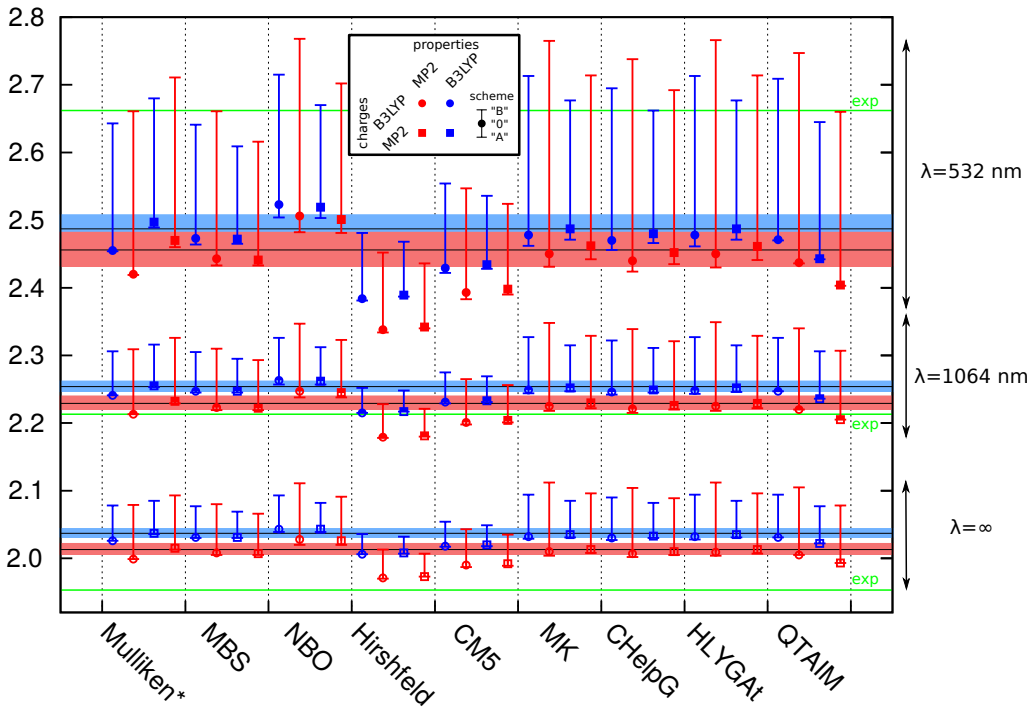

Fig. 4: Effect of charge definition on the n_x value of MNA (values for λ=1064 nm were shifted by +0.15 for clarity). Red (MP2) and blue (B3LYP) ribbons give the range of reference results, *i.e.* obtained using PBC-Mulliken charges, and their spread when scaling the charges by 0.95 (lower value) or 1.05 (higher value) while the solid black lines correspond to the unscaled charges. For each charge definition and level of approximation for calculating the charges and properties, the results take the form of a point with bounded vertical lines. The 0-th cycle results are represented by the full symbols, whereas the lower and upper bars correspond to results obtained with converged point charge values within schemes A and B, respectively. Red/blue symbols are used when the molecular properties are evaluated at the MP2/B3LYP level. Squares and circles indicate the method used for computing the charges, MP2 or B3LYP, respectively. Green lines represent the experimental values.

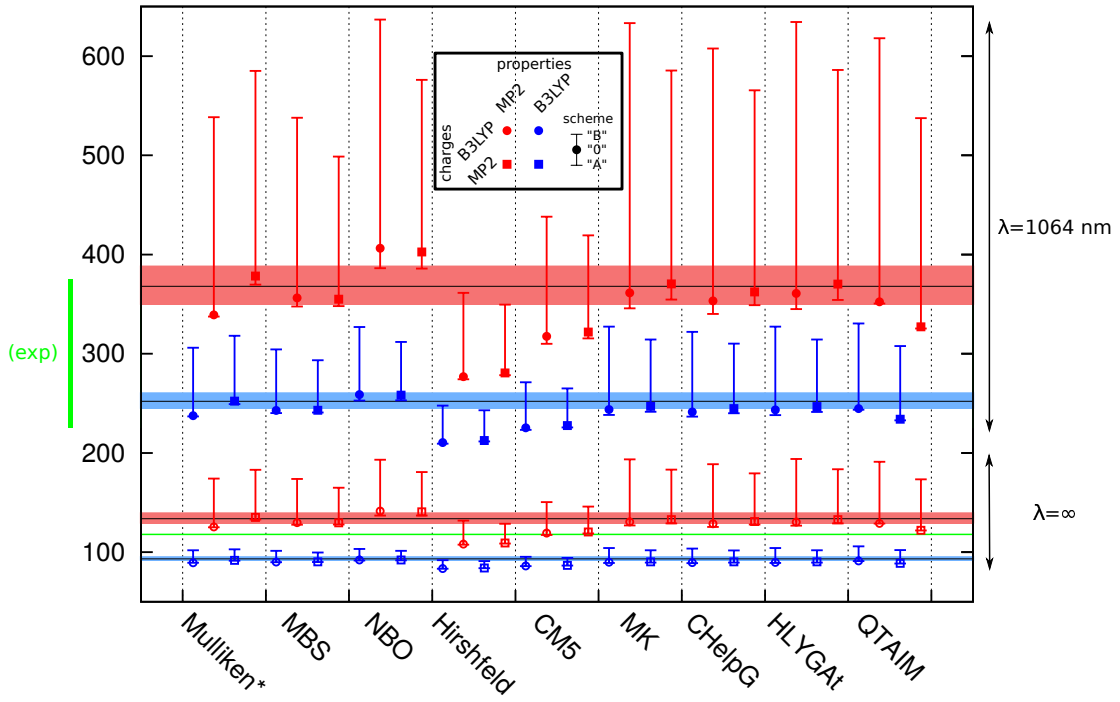

Fig. 5: Effect of charge definition on $-\chi^{(2)}_{111}$ (in pm/V) of MNA. See the Caption of Fig. 4 for the figure legend.

References

[1] D. Stueber, F. N. Guenneau, and D. M. Grant, *J. Chem. Phys.*, 2001, **114**(21), 9236–9243.

[2] D. Solis and M. Ferraro, *Theor. Chem. Acc.*, 2000, **104**(3-4), 323–326.

[3] D. Solıs, M. Ferraro, and J. Facelli, *J. Mol. Struct.*, 2002, **602**, 159–164.

[4] J. P. Foster and F. Weinhold, *J. Am. Chem. Soc.*, 1980, **102**, 7211–7218.

[5] C. M. Breneman and K. B. Wiberg, *J. Comp. Chem.*, 1990, **11**, 361–373.

[6] N. Di Fiori, A. M. Orendt, M. Caputo, M. Ferraro, and J. Facelli, *Magn. Reson. Chem.*, 2004, **42**(S1), S41–S47.

[7] J. Weber and J. S. auf der Günne, *Phys. Chem. Chem. Phys.*, 2010, **12**(3), 583–603.

[8] R. Bjornsson and M. Bühl, *J. Chem. Theory Comput.*, 2012, **8**(2), 498–508.

[9] U. C. Singh and P. A. Kollman, *J. Comp. Chem.*, 1984, **5**, 129–145.

[10] N. Özcan, T. Kortelainen, V. Golovanov, T. T. Rantala, and J. Vaara, *Phys. Rev. B*, 2010, **81**(23), 235202.

[11] L. C. Menikarachchi and J. A. Gascón, *Curr. Top. Med. Chem.*, 2010, **10**(1), 46–54.

[12] P. Söderhjelm, F. Aquilante, and U. Ryde, *J. Phys. Chem. B*, 2009, **113**(32), 11085–11094.

[13] D. E. Vanpoucke, J. Oláh, F. De Proft, V. Van Speybroeck, and G. Roos, *J. Chem. Inf. Model.*, 2015, **55**(3), 564–571.

[14] E. E. Dahlke and D. G. Truhlar, *J. Chem. Theory Comput.*, 2007, **3**(4), 1342–1348.

[15] P. Bygrave, N. Allan, and F. Manby, *J. Chem. Phys.*, 2012, **137**(16), 164102.

[16] S. L. Price, *Chem. Soc. Rev.*, 2014, **43**(7), 2098–2111.

[17] K. Coutinho and S. Canuto, *Adv. Quantum Chem.*, 1997, **28**, 89.

[18] K. Coutinho, S. Canuto, and M. Zerner, *J. Chem. Phys.*, 2000, **112**, 9874.

[19] M. Hidalgo Cardenuto and B. Champagne, *J. Chem. Phys.*, 2014, **141**(23), 234104.

[20] J. Quertinmont, B. Champagne, F. Castet, and M. Hidalgo Cardenuto, *J. Phys. Chem. A*, 2015.

[21] S. Höfener, A. S. P. Gomes, and L. Visscher, *J. Chem. Phys.*, 2013, **139**(10), 104106.

[22] T. Seidler, K. Stadnicka, and B. Champagne, *J. Chem. Phys.*, 2013, **139**, 114105.

[23] T. Seidler, K. Stadnicka, and B. Champagne, *J. Chem. Theory Comput.*, 2014, **10**, 2114–2124.

[24] T. Seidler, K. Stadnicka, and B. Champagne, *Adv. Optical Mater*, 2014, **2**, 1000–1006.

[25] F. L. Hirshfeld, *Theoret. Chim. Acta (Berl.)*, 1977, **44**, 129–138.

[26] R. W. Bader, *Atoms in Molecules: A Quantum Theory*, Oxford University Press, 1994.

[27] J. A. Montgomery Jr, M. J. Frisch, J. W. Ochterski, and G. A. Petersson, *J. Chem. Phys.*, 2000, **112**(15), 6532–6542.

[28] H. Hu, Z. Lu, and W. Yang, *J. Chem. Theory and Comput.*, 2007, **3**, 1004–1013.

[29] A. V. Marenich, S. V. Jerome, C. J. Cramer, and D. G. Truhlar, *J. Chem. Theory and Comput.*, 2012, **8**, 527–541.

[30] H. Reis, M. G. Papadopoulos, C. Hättig, J. G. Ángyán, and R. W. Munn, *J. Chem. Phys.*, 2000, **112**(14), 6161–6172.

[31] M. Hurst and R. Munn in *Organic Materials for Nonlinear Optics;* The Royal Society of Chemistry, London, 1989.

[32] H. Reis, M. G. Papadopoulos, and R. Munn, *J. Chem. Phys.*, 1998, **109**(16), 6828–6838.

[33] M. J. Frisch, G. W. Trucks, H. B. Schlegel, G. E. Scuseria, M. A. Robb, J. R. Cheeseman, G. Scalmani, V. Barone, B. Mennucci, G. A. Petersson, H. Nakatsuji, M. Caricato, X. Li, H. P. Hratchian, A. F. Izmaylov, J. Bloino, G. Zheng, J. L. Sonnenberg, M. Hada, M. Ehara, K. Toyota, R. Fukuda, J. Hasegawa, M. Ishida, T. Nakajima, Y. Honda, O. Kitao, H. Nakai, T. Vreven, J. A. Montgomery, Jr., J. E. Peralta, F. Ogliaro, M. Bearpark, J. J. Heyd, E. Brothers, K. N. Kudin, V. N. Staroverov, R. Kobayashi, J. Normand, K. Raghavachari, A. Rendell, J. C. Burant, S. S. Iyengar, J. Tomasi, M. Cossi, N. Rega, J. M. Millam, M. Klene, J. E. Knox, J. B. Cross, V. Bakken, C. Adamo, J. Jaramillo, R. Gomperts, R. E. Stratmann, O. Yazyev, A. J. Austin, R. Cammi, C. Pomelli, J. W. Ochterski, R. L. Martin, K. Morokuma, V. G. Zakrzewski, G. A. Voth, P. Salvador, J. J. Dannenberg, S. Dapprich, A. D. Daniels, O. Farkas, J. B. Foresman, J. V. Ortiz, J. Cioslowski, and D. J. Fox, Gaussian 09 Revision A.02.

[34] A. E. Whitten, P. Turner, W. T. Klooster, R. O. Piltz, and M. A. Spackman, *J. Phys. Chem. A*, 2006, **110**, 8763–8776.

[35] K. B. Wiberg and P. R. Rablen, *J. Comput. Chem.*, 1993, **14**(12), 1504–1518.

[36] G. F. Lipscomb, A. F. Garito, and R. S. Narang, *J. Chem. Phys.*, 1981, **75**(3), 1509–1516.

[37] A. E. Goeta, C. C. Wilson, J. C. Autino, J. Ellena, and G. Punte, *Chem. Mater.*, 2000, **12**(11), 3342–3346.

[38] A. Fkyerat, A. Guelzim, E. Baert, W. Paulus, G. Heger, J. Zyss, and A. Perigaud, *Acta Crystallogr. Sect. B-Struct. Sci.*, 1995, **51**(2), 197–209.

[39] T. Seidler, K. Stadnicka, and B. Champagne In *4th International Congress in Advances in Applied Physics and Materials Science (APMAS 2014)*, Vol. 1653, p. 020096. AIP Publishing, 2015.

[40] K. Sutter, C. Bosshard, W. Wang, G. Surmely, and P. Günter, *Applied physics letters*, 1988, **53**(19), 1779–1781.

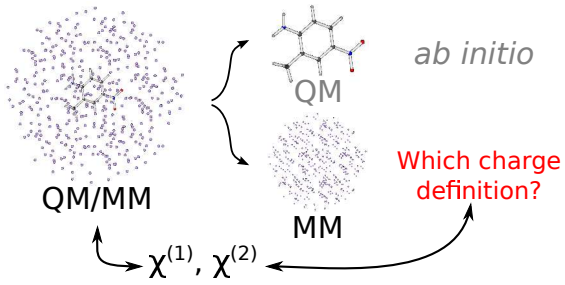

TOC phrase: Crystal optical susceptibilities are probes to assess the performance of the charge definition employed to describe the crystal polarizing field.